Coastal Dynamics 2017
Paper No. 221

3D PHASE-AVERAGED MODELLING OF THE HYDRODYNAMICS OF A DISSIPATIVE BEACH UNDER ENERGETIC CONDITIONS

Thomas Guérin[1] and Xavier Bertin[1]

Abstract

This study presents the analysis of the 3D hydrodynamics of a dissipative beach (Saint-Trojan, France) under energetic wave conditions. A field campaign was carried out in early February 2017 and the analysis of the data is complemented with 3D hydrodynamic numerical hindcast using the unstructured grid modelling system SCHISM-WWM-II with a vortex force formalism. Numerical results are compared with field measurements and an accuracy corresponding to the state of the art for this type of coastal environment is obtained for water levels, wave parameters, bottom currents, and wave setup. The comparison between 3D and 2DH runs then revealed the potential underestimation of the 2DH predicted setup, particularly under energetic wave conditions. This difference is explained through the contribution of the vertical circulation that develop in the surfzone and which is simulated only in 3D.

Key words: hydrodynamics, dissipative beach, 3D numerical modelling, vortex force, energetic conditions, setup

1. Introduction

When reaching the shoreline, the breaking of energetic short waves can have several major impacts on the coastal zone such as for instance the increase in mean sea level at the shore (i.e. the wave setup), or the offshore sediment transport due to the wave-induced seaward bottom current (i.e. the undertow) which can significantly contribute to beach erosion. By considering a two-dimensional (vertically integrated) phase-averaged approach, Longuet-Higgins and Stewart (1964) analytically showed that an increase of the free surface elevation is induced by a negative gradient of radiation stress, the latter term being defined by the authors as the excess flux of momentum due to the presence of waves. In order to also explain the wave-induced circulation along the vertical, three-dimensional approaches have then been developed by several authors (e.g. Mellor, 2003; Mc Williams et al., 2004; Ardhuin et al., 2008b), although some intense debate took place about the advantages and drawbacks of each approach. In 2003, Mellor proposed a formulation to compute wave radiation stresses in 3D based on an Eulerian mean approach, but this formulation was shown to be incomplete by Ardhuin et al. (2008a), which then led Mellor to propose a corrected formulation (Mellor, 2008). Ardhuin et al. (2008b) proposed their own theory based on a generalized Lagrangian mean approach (Andrews and McIntyre, 1978). While Ardhuin et al. (2008b) showed that the radiation stress approach in 3D could lead to spurious velocities in adiabatic conditions, Moghimi et al. (2013) showed that both approaches performed reasonably in conditions dominated by wave dissipation such as surf zones.

2. Study area and field campaign

The Saint-Trojan beach is located in the central part of the French Atlantic coast, along the South-West part of the Oléron Island (Fig. 1). This beach is wave-dominated and presents a gentle slope ranging between less than 0.002 offshore and about 0.015 in the intertidal area, leading to a dissipative morphology (Bertin et al., 2008). This beach is also characterized by a macrotidal regime, with a tidal range varying between about 2 and 5.5 m.

[1]UMR 7266 LIENSs – CNRS, La Rochelle University, 2 rue Olympe de Gouges, 17000 La Rochelle, France.
thomas.guerin@univ-lr.fr ; xavier.bertin@univ-lr.fr

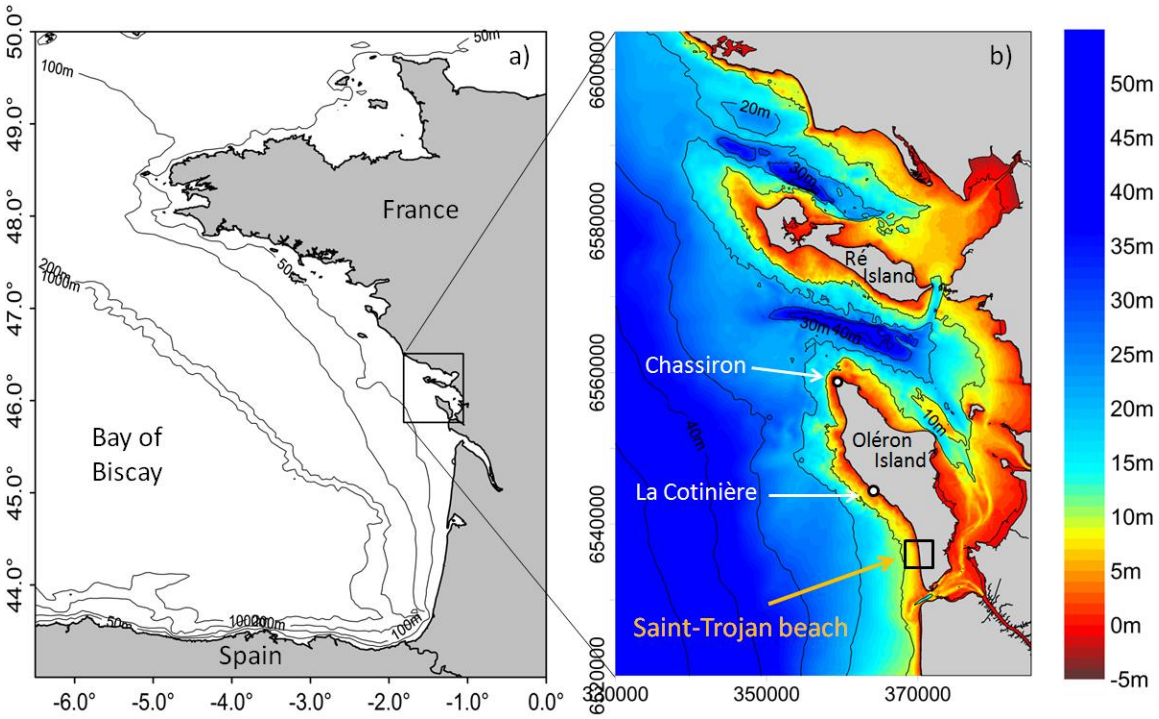

Figure 1. Location of the study area: the Saint-Trojan beach. Coordinates of b) are in meters (*Lambert-93* projection).

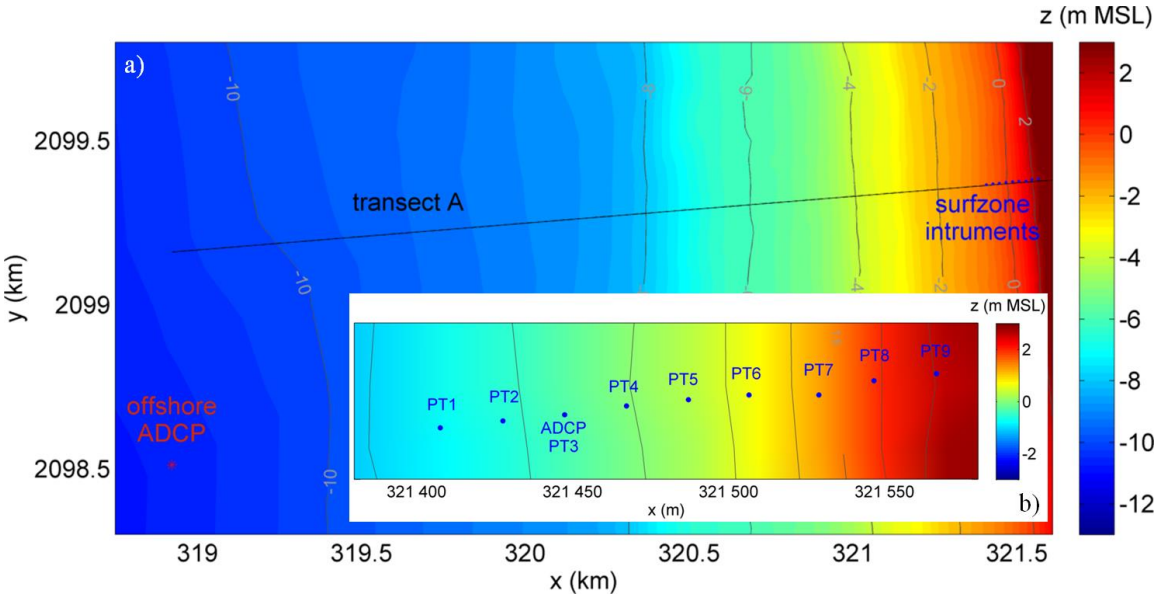

Figure 2. a) Bathymetry of the St Trojan beach with the location of the deployed instruments and the transect considered in the simulations. b) Zoom on the intertidal area. Coordinates are in meters (*Lambert 2 étendue* projection).

The field campaign took place during early February 2017 with the deployment of an offshore current profiler (ADCP) in a water depth of about 11 m with respect to the mean sea level (MSL), 9 pressure transducers in the intertidal zone, and a second ADCP at the PT3 station (Fig. 2). The measurement period covers three tidal cycles during a period of mean tides (i.e. tidal range between 3.5 and 4 m), from 1st to the 3rd of February. The offshore wave conditions during this period can be classified as energetic since the significant wave height (Hs) varied between 2 and 4 m at the offshore ADCP, with a

peak period (Tp) of about 14 s over the main part of the measurement period. The measured water levels, wave parameters, and bottom currents are analyzed in more details in section 4, where comparisons between measurements and model results are done.

3. Numerical Modelling System

3.1. *Hydrodynamic model*

The core of the modelling system used in this study is the Semi-implicit Cross-scale Hydroscience Integrated System Model (SCHISM) of Zhang et al. (2016), which is an upgrade from the model SELFE of Zhang and Baptista (2008). It is a 3D, parallelized, unstructured-grid model and presents the main feature of combining an Eulerian-Lagrangian method to treat the advection in the momentum equations with semi-implicit schemes, which relaxes the numerical stability constraints of the model. In the present study the hydrodynamic time step is 15 s, while the spatial resolution ranges between 4.5 km at the offshore boundary down to 20 m in the study area, and 11 sigma levels are used for the vertical discretization. The tidal forcing is computed with the 16 main tidal constituents, and the wind and pressure sea-level fields from the Climate Forecast System Reanalysis (CFSR) with 1 h time resolution are used for the atmospheric forcing.

3.2. *Wave model*

We use the latest version of the Wind Wave Model of Roland et al. (2012) which is a third generation, spectral (i.e. phase-averaged) wave model. It simulates gravity waves generation and propagation by solving the wave action equation (Komen et al., 1996), while it is fully coupled to SCHISM and share the same domain-decomposition. The time step is also 15 s, and 30 frequencies and 30 directions are considered for the wave spectral discretization. The wave forcing is obtained from the hindcast of Bertin et al. (2013) which used the spectral wave model WaveWatch-III forced with the CFSR wind fields. In order to correctly represent the 3D wave-induced currents in our modelling system, the vortex force formalism introduced by Ardhuin et al. (2008b) has been implemented following Bennis et al. (2011). Moreover, the energy dissipation due to depth-induced wave breaking is computed with the model of Thornton and Guza (1983).

4. Model results

A good agreement is obtained when comparing measured and simulated water level and wave parameters (Hs, Tp, and Tm02) at the offshore ADCP location (Fig. 3), with an accuracy corresponding to the state of the art for this type of coastal environment and conditions. The model results for the water level and the significant wave height at the intertidal stations are also satisfactory (Fig. 4-5), the latter parameter being here mainly controlled by the breaking index which is adjusted to 0.55 in our simulation.

As for the simulated bottom cross-shore current in the surfzone, which is a key outcome in this study since it (partly) allows validating the vortex force formalism implemented in the model, a good match is obtained when compared to the measurement at the ADCP station (Fig. 6). The same comparison at the offshore ADCP station also appears satisfactory (Fig. 7), with an unchanged root-mean-square error (RMSE) of 0.07 m/s compared to the surfzone station, though the cross-shore current at this offshore location is mainly tidally controlled.

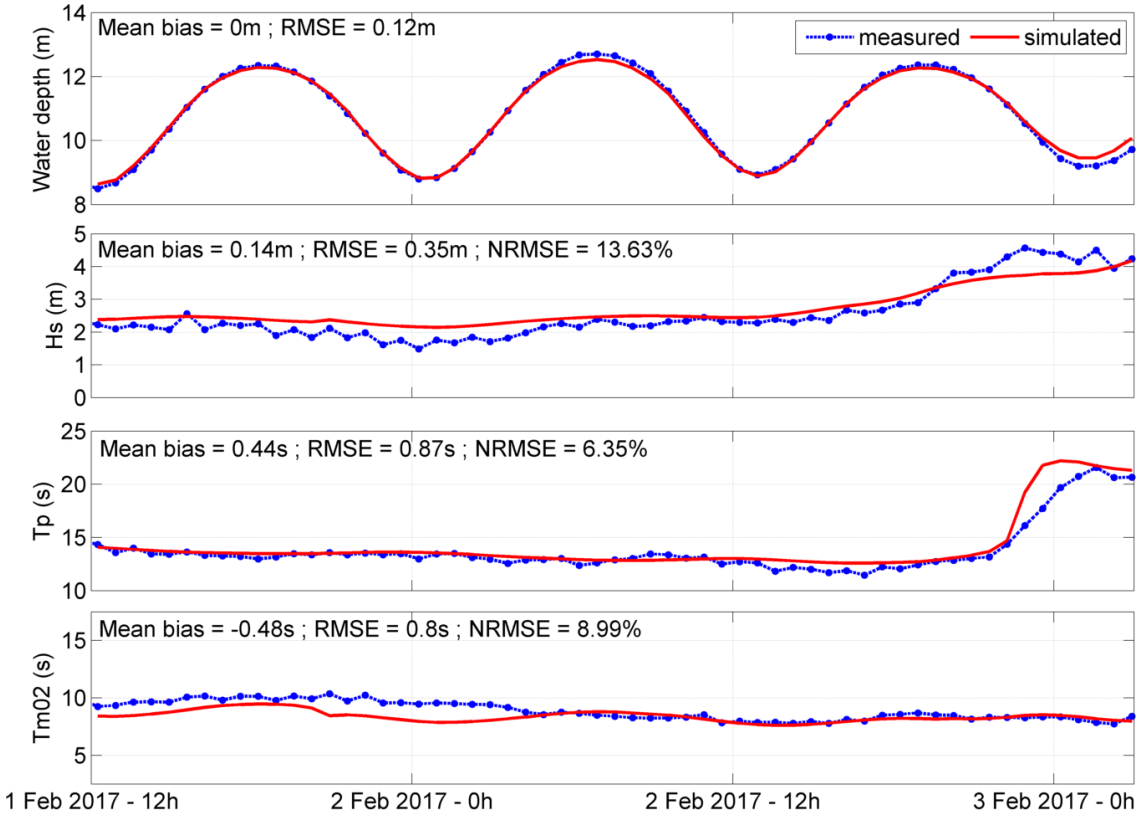

Figure 3. Comparison of measurements and model results at the offshore ADCP, for water level, significant wave height (Hs), peak period (Tp), and Tm02 period.

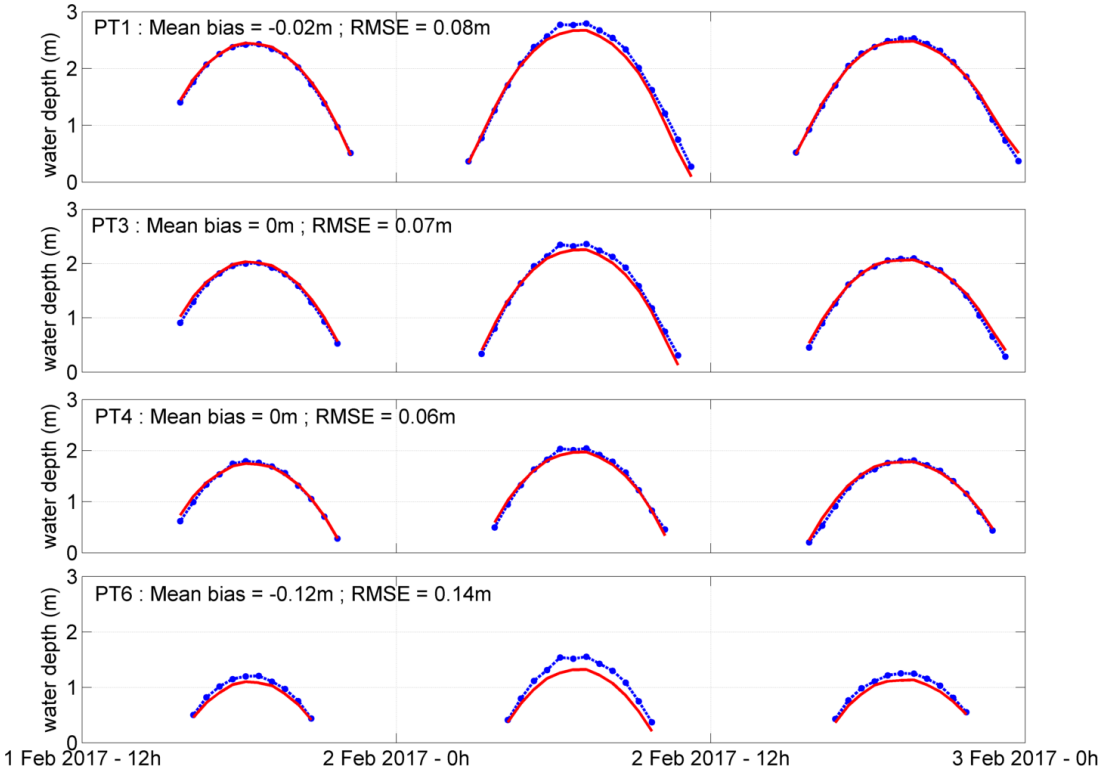

Figure 4. Comparison of measured and simulated water level at the intertidal stations.

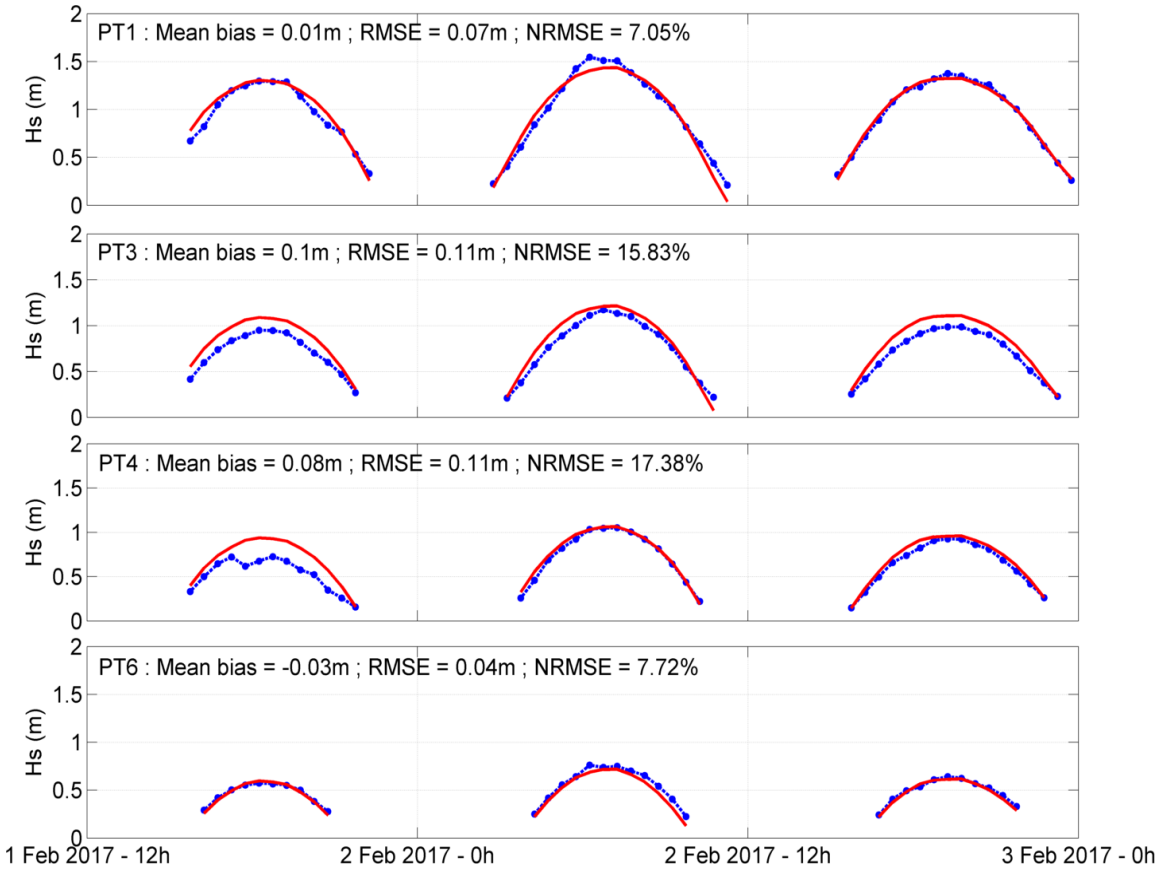

Figure 5. Comparison of measured and simulated significant wave height (Hs) at the intertidal stations.

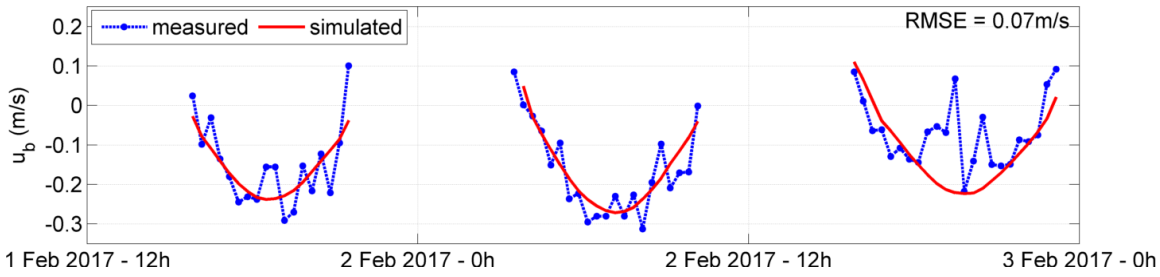

Figure 6. Comparison of measured and simulated bottom cross-shore velocity (u_b) at the PT3 station (0.47 m from the bottom).

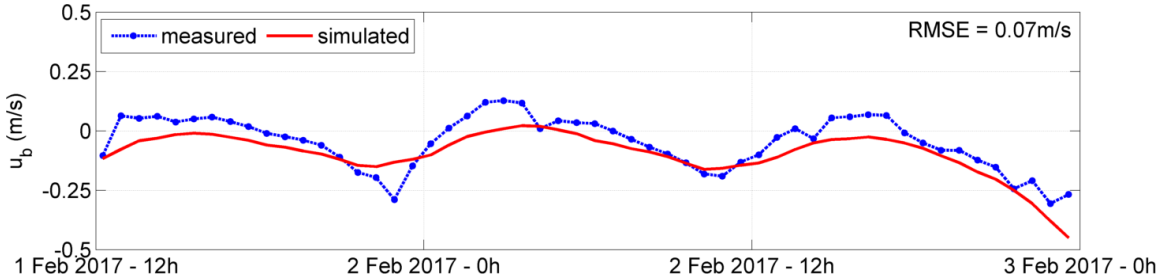

Figure 7. Comparison of measured and simulated bottom cross-shore velocity (u_b) at the offshore ADCP (2.15 m from the bottom).

Unlike other wave and hydrodynamic parameters, wave setup cannot be measured directly and its estimation requires a special care in order to perform consistent model-data comparisons. A first option would be to subtract from measured water levels a tidal prediction computed at the nearest tide gauge but this approach suffers two shortcomings. First, the tidal prediction has its own errors, which could impact setup estimates by a few centimeters. Second, the atmospheric storm surge cannot be removed while it can represent a large part of the water level anomaly. Alternatively, we proposed a new approach where we estimate a so-called "relative setup", where we remove the water level measured at the offshore ADCP from the water level measured at each sensor of the intertidal zone. Given that the ADCP was located outside the surfzone, this method allows removing both the tidal signal and the atmospheric storm surge from the water levels measured in the intertidal zone. The same approach was applied to model results, in order to guaranty a consistent model/data comparison.

Comparisons between relative setup computed from measured and simulated water levels are shown on Fig. 8. Though some discrepancies remain between the different sensors, a satisfactory general result is obtained with an overall mean bias and RMSE of about -0.5 cm and 5 cm respectively. We specify that, because of a drifting problem concerning some pressure transducers, only three sensors were retained to compute realistic values of relative setup.

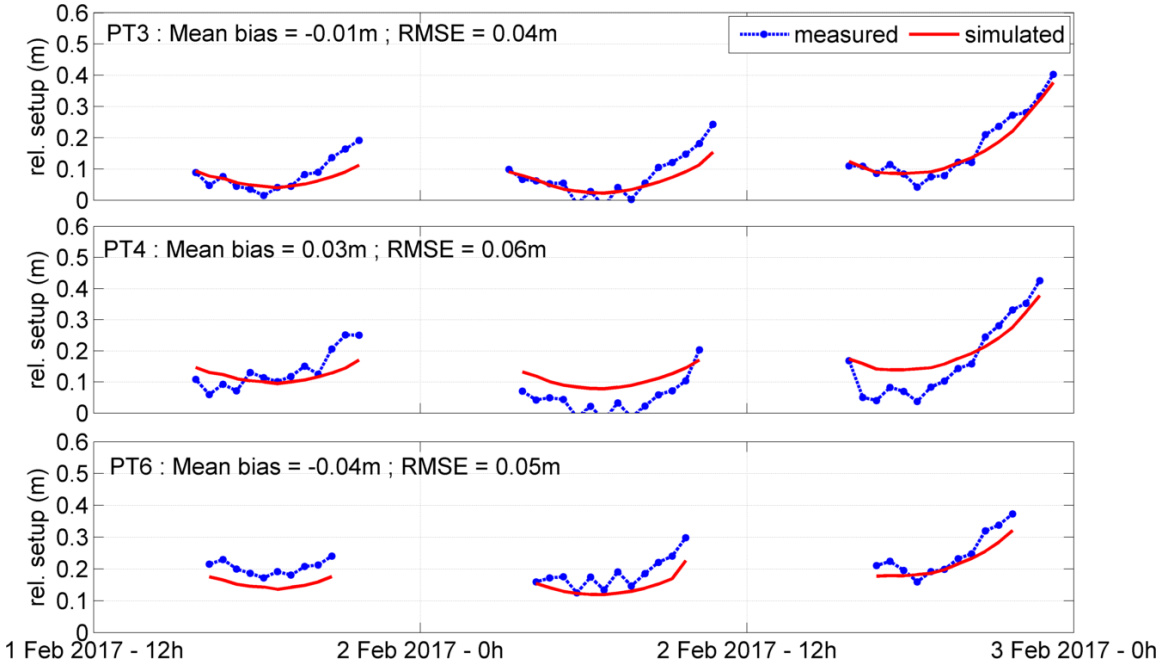

Figure 8. Comparison between measured and simulated relative setup at the intertidal stations, computed as the local water level minus the water level at the offshore ADCP.

5. Impact of the wave-induced 3D circulation on the setup

Simulations with only waves (i.e. no tidal and atmospheric forcings) are now considered in order to isolate the contribution on the setup of the wave-induced 3D circulation resulting from the use of the vortex force formalism in our modelling system. More precisely, three different configurations of the model are considered: a 3D one with a vertically-varying distribution profile of momentum due to wave breaking (i.e. a hyperbolic cosine function is used for the vertical profile as in Uchiyama et al. (2010), that we (abusively) refer as realistic profile in the following), a 3D one with a homogeneous vertical distribution allowing us to get a vanishing cross-shore wave-induced current along the vertical, and a 2DH one. A first comparison can be to simply consider the realistic 3D one and the 2DH one, but comparing also the two 3D simulations allows us to analyze only the impact of the wave-induced 3D circulation on the setup. There are indeed other differences between 3D and 2D configurations, such as the turbulence closure

model which is absent in the 2D mode and is linked to the bottom friction computation in the hydrodynamic module.

Three different input wave conditions are selected by taking a significant wave height of 4, 6, and 8 m at the offshore boundary, while keeping a peak period of 14 sec (as during the main part of the field campaign). Such conditions result in a significant wave height of the order of 2.5, 3.5, and 4.5 m at the breaking point, respectively. The steady-state surface elevation (or setup) simulated at St Trojan beach for the three wave conditions and the three model configurations is plotted along a cross-shore transect (Fig. 9-11 a)), together with the respective setup increase between the realistic 3D simulation and the two others (Fig. 9-11 b)). First, these figures show that the setup at the shoreline is higher for the realistic 3D configuration than for the two other configurations, while this difference increases with Hs. This increase in setup between the different configurations reaches a maximum of about 10, 20, and 30 % for an incident Hs of 4, 6, and 8 m respectively. Second, it can be seen that the setup simulated with the vertically homogeneous 3D configuration and the 2D one are close, which ensures us that the differences previously mentioned between 3D and 2D configurations (i.e. excluding the wave-induced 3D circulation) are weak. We can thus be confident when saying that the main effect responsible for the setup increase between the realistic 3D configuration and the 2D one is due to the wave-induced 3D circulation in the breaking zone.

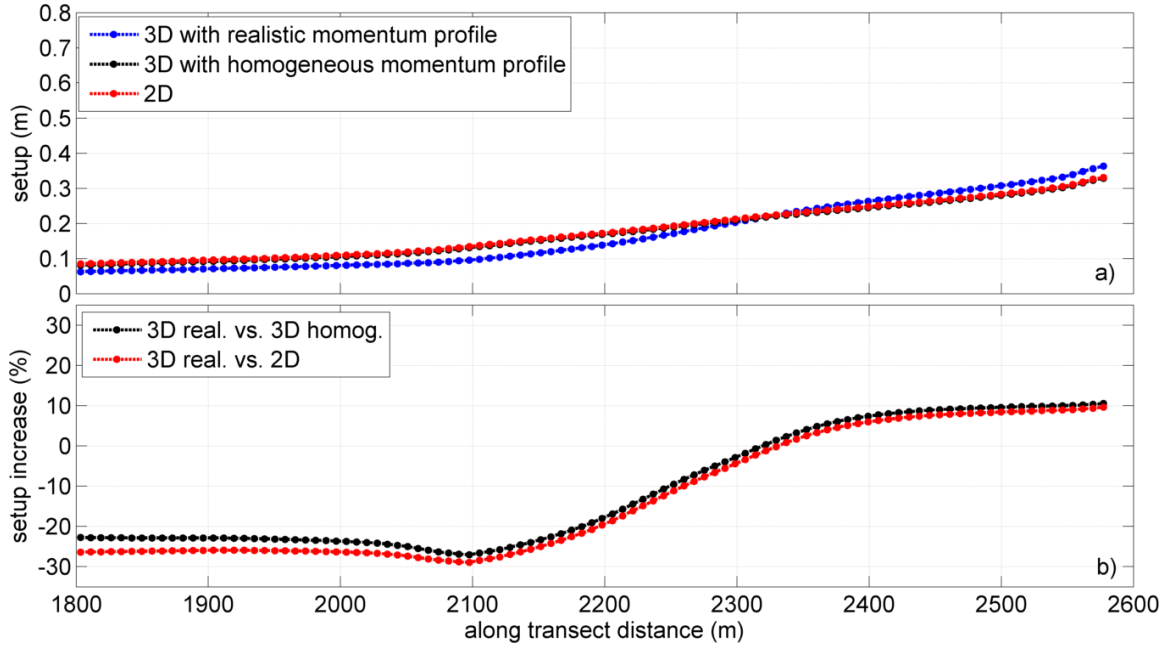

Figure 9. Simulations with Hs = 4 m and Tp = 14 sec at the offshore boundary: a) setup 3D-simulated with a vertically-varying (or realistic) distribution profile of momentum due to wave breaking (blue curve), with a vertically-homogeneous distribution (black curve), and 2D-simulated (red curve); b) setup increase between the different simulations.

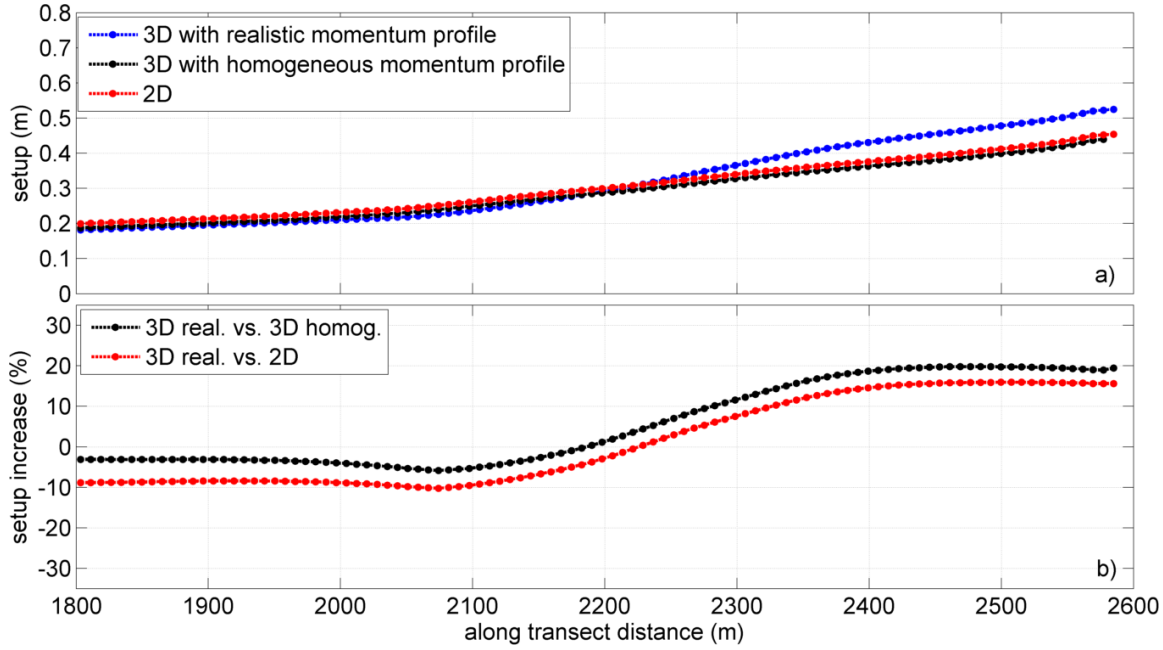

Figure 10. Simulations with Hs = 6 m and Tp = 14 sec at the offshore boundary.

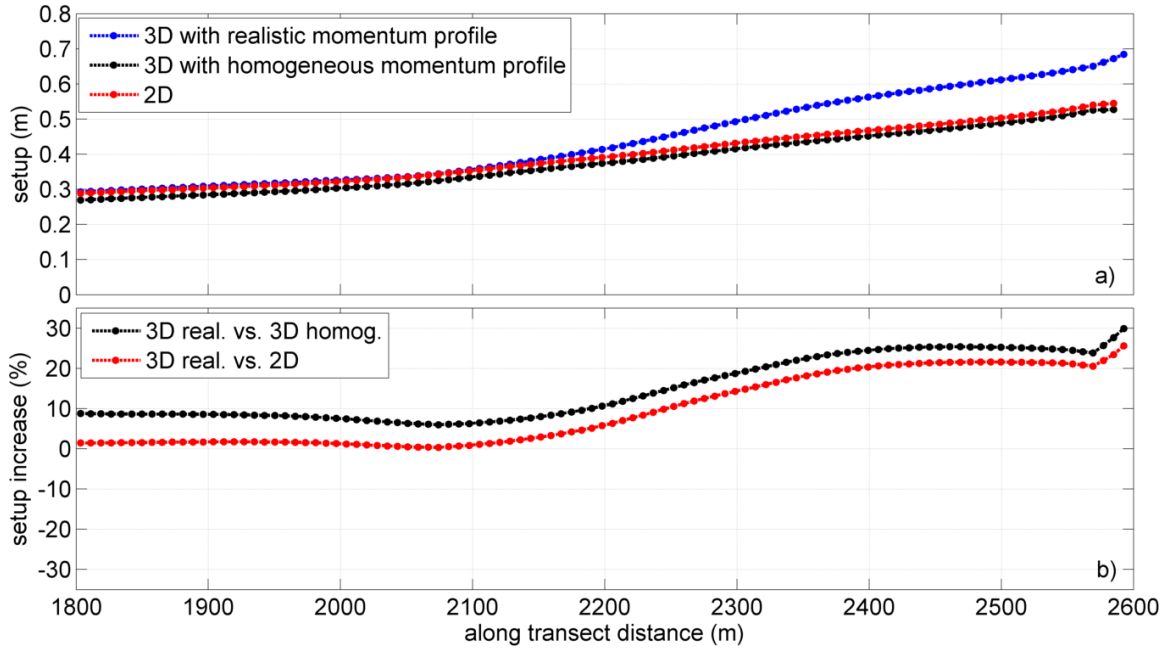

Figure 11. Simulations with Hs = 8 m and Tp = 14 sec at the offshore boundary.

6. Discussion and conclusion

Based on an analytical depth-averaged approach, the study of Apotsos et al. (2007) already highlighted the potential increase of the setup due to the presence of the undertow because it increases the onshore-directed component of the bottom stress. The present study expands this result to the impact of the complete wave-induced 3D circulation in the surfzone on the setup prediction. More precisely, a preliminary analysis of the different terms of the momentum equation revealed that this setup increase between 3D and 2DH runs was mainly due to the horizontal cross-shore advection term and, in a lesser extent, to the vertical advection and

vertical viscosity terms. This study also shows that the difference concerning the 3D and the 2DH predicted setup increases significantly as the incoming wave height increases.

Future tests would be to analyze the joint effect of for instance the wave-induced turbulence (as discussed in Bennis et al., 2014) and the beach characteristics (e.g. slope, bedforms) on the setup prediction. Comparison between the phase-averaged approach proposed in this study with phase-resolving models (e.g. Nicolae Lerma et al., 2017) could also be relevant.

Acknowledgements

This work was done in the scope of the EVEX project, funded by the Poitou-Charentes region (France). We warmly thank Anouk de Bakker and Thibault Coulombier for their participation during the field work. The SCHISM developers are also greatly acknowledged.

References

Andrews, D.G., McIntyre, M.E., 1978. An exact theory of nonlinear waves on a Lagrangian-mean flow. *Journal of Fluid Mechanics*. 89: 609–646.

Apotsos, A., Raubenheimer, B., Elgar, S., Guza, R.T., Smith, J.A., 2007. Effects of wave rollers and bottom stress on wave setup. *Journal of Geophysical Research*, 112, C02003.

Ardhuin, F., Jenkins, A.D., Belibassakis, K., 2008a. Commentary on the threedimensional current and surface wave equations' by George Mellor. *Journal of Physical Oceanography*, 38 : 1340–1349.

Ardhuin, F., Rascle, N., Belibassakis, K.A., 2008b. Explicit wave-averaged primitive equations using a generalized Lagrangian mean. *Ocean Modelling*, 20: 35-60.

Bennis, A.-C., Ardhuin, F., and Dumas, F., 2011. On the coupling of wave and three-dimensional circulation models: Choice of theoretical framework, practical implementation and adiabatic tests. *Ocean Modelling*, 40: 260-272.

Bennis, A.-C., Dumas, F., Ardhuin, F., Blanke, B., 2014. Mixing parameterization: Impacts on rip currents and wave set-up. *Ocean Engineering*, 84: 213-227.

Bertin, X., Castelle, B., Chaumillon, E., Butel, R., Quique, R., 2008. Longshore transport estimation and inter-annual variability at a high-energy dissipative beach: St. Trojan beach, SW Oléron Island, France. *Continental Shelf Research*, 28: 1316-1332.

Bertin, X., Prouteau, E., Letretel, C., 2013. A significant increase in wave height in the North Atlantic Ocean over the 20th century. *Global and Planetary Change*, 106: 77-83.

Komen, G.J., Cavaleri, L., Donelan, M., Hasselmann, K., Hasselmann, S., Janssen, P.A.E.M., 1996. *Dynamics and Modelling of Ocean Waves*, Cambridge University Press.

Longuet-Higgins, M.S., and Stewart, R.W., 1964. Radiation stress in water waves, a physical discussion with applications. *Deep Sea Research*, 11: 529–563.

Longuet-Higgins, M.S., 1967. On the wave-induced difference in mean sea level between the two sides of a submerged breakwater. *Journal of Marine Research*, 25: 148–153

McWilliams, J.C., Restrepo, J.M., Lane, E.M., 2004. An asymptotic theory for the interaction of waves and currents in coastal waters. *Journal of Fluid Mechanics*, 511: 135-178.

Mellor, G., 2003. The three-dimensional current and surface wave equations. Journal of Physical Oceanography, 33: 1978–1989.

Mellor, G., 2008. The depth-dependent current and wave interaction equations: a revision. *Journal of Physical Oceanography*, 38: 2587–2596.

Mellor, G., 2016. On theories dealing with the interaction of surface waves and ocean circulation. *Journal of Geophysical Research: Oceans*, 121: 4474-4486.

Moghimi, S., Klingbeil, K., Gräwe, U, Burchard, H., 2013. A direct comparison of a depth-dependent Radiation stress formulation and a Vortex force formulation within a three-dimensional coastal ocean model. *Ocean Modelling*, 70: 132-144.

Nicolae Lerma, A., Pedreros, R., Robinet, A., Sénéchal, N., 2017. Simulating wave setup and runup during storm conditions on a complex barred beach. *Coastal Engineering*, 123: 29-41.

Roland, A., Zhang, Y.J., Wang, H.V., Meng, Y., Teng, Y.C., Maderich, V., Brovchenko, I., Dutour-Sikiric, M., Zanke, U., 2012. A fully coupled 3D wave-current interaction model on unstructured grids. *Journal of Geophysical* Research, 117, C00J33.

Thornton, E.B., and Guza, R.T., 1983. Transformation of wave height distribution. Journal of Geophysical Research, 88(C10): 5925–5938.

Uchiyama, Y., McWilliams, J.C., Shchepetkin, A.F., 2010. Wave-current interaction in an oceanic circulation model with a vortex-force formalism: Application to the surf zone. *Ocean Modelling*, 34: 16–35.

Zhang, Y.J., Ye, F., Stanev, E.V., Grashorn, S., 2016. Seamless cross-scale modeling with SCHISM. *Ocean Modelling*, 102: 64–81.

Zhang, Y., and Baptista, A.M., 2008. SELFE: A semi-implicit Eulerian–Lagrangian finite-element model for cross-scale ocean circulation. *Ocean Modelling*, 21: 71–96.